Time-Resolved Spectroscopic Studies of B12 Coenzymes: The Identification of a Metastable Cob(III)alamin Photoproduct in the Photolysis of Methylcobalamin

ARTICLE *in* JOURNAL OF THE AMERICAN CHEMICAL SOCIETY · APRIL 1998

Impact Factor: 12.11 · DOI: 10.1021/ja974024q

6 AUTHORS, INCLUDING:

Joseph T Jarrett
University of Hawai'i System
49 PUBLICATIONS **4,859** CITATIONS
SEE PROFILE

Stuart Pullen
Eisai Japan
13 PUBLICATIONS **349** CITATIONS
SEE PROFILE

Rowena Green Matthews
University of Michigan
172 PUBLICATIONS **13,349** CITATIONS
SEE PROFILE

Roseanne J Sension
University of Michigan
108 PUBLICATIONS **2,401** CITATIONS
SEE PROFILE

Time-Resolved Spectroscopic Studies of B_{12} Coenzymes: The Identification of a Metastable Cob(III)alamin Photoproduct in the Photolysis of Methylcobalamin

Larry A. Walker, II,[†] Joseph T. Jarrett,[‡] Neil A. Anderson,[†] Stuart H. Pullen,[†] Rowena G. Matthews,[‡,§] and Roseanne J. Sension*[,†]

Contribution from the Department of Chemistry, Department of Biological Chemistry, and Biophysics Research Division, University of Michigan, Ann Arbor, Michigan 48109-1055

Received November 25, 1997

Abstract: Ultrafast transient absorption spectroscopy has been used to investigate the primary photochemistry of methylcobalamin. Approximately 27% of the initially excited methylcobalamin undergoes a bond homolysis on a subpicosecond time scale. The remaining 73% forms a metastable photoproduct with a spectrum similar to that of cob(III)alamin compounds. The ultraviolet absorption spectrum of the metastable photoproduct exhibits a prominent γ-band at 340 nm, characteristic of a cob(III)alamin with a very weak axial ligand. The metastable photoproduct recovers to the ground electronic state of methylcobalamin on a 1.2 ± 0.5 ns time scale, leaving only cob(II)alamin (and presumably methyl radical) at 9 ns. The primary photochemical yield of cob(II)alamin is determined largely by the branching ratio between the two photoproduct channels. A 40 ps transient absorption difference spectrum of methylcobalamin bound to methionine synthase indicates that the branching ratio and initial production of cob(II)alamin is not changed in the enzyme-bound cofactor. The substantial photolysis protection afforded by the enzyme must be attributed to structural and electronic effects which enhance the intrinsic rate of recombination of the radical pair, rather than to suppression of primary bond homolysis.

Introduction

The B_{12}-dependent enzymes may be classified into two broad categories: methyltransferase enzymes, where the B_{12} cofactor is methylcobalamin (shown in Figure 1) or a related methylcorrinoid derivative, and mutase enzymes, where the B_{12} cofactor is adenosylcobalamin. The mechanism in the methyltransferase enzymes involves formal heterolytic cleavage of the carbon−cobalt bond forming cob(I)alamin and a methyl cation.[1,2] The mechanism in the mutase enzymes involves homolytic cleavage of the carbon−cobalt bond to form cob(II)alamin and an adenosyl radical (Ado•).[2,3] Currently 12 distinct mutase enzymes and 8 distinct methyltransferase enzymes are known.[2,4−6] One mutase (methylmalonyl-CoA mutase) and one methyltransferase (methionine synthase) are known to occur in humans.

An important open question in B_{12} catalysis addresses the nature of the protein−coenzyme interaction, i.e., how the protein weakens the carbon−cobalt bond to allow facile bond cleavage. Recent crystal structures have demonstrated that the dimethylbenzimidazole (DMB) base is displaced in methionine synthase and methylmalonyl-CoA mutase while a histidine residue from the protein provides the lower axial ligand to the cobalt.[7,8] This observation has provided some insight into possible protein−

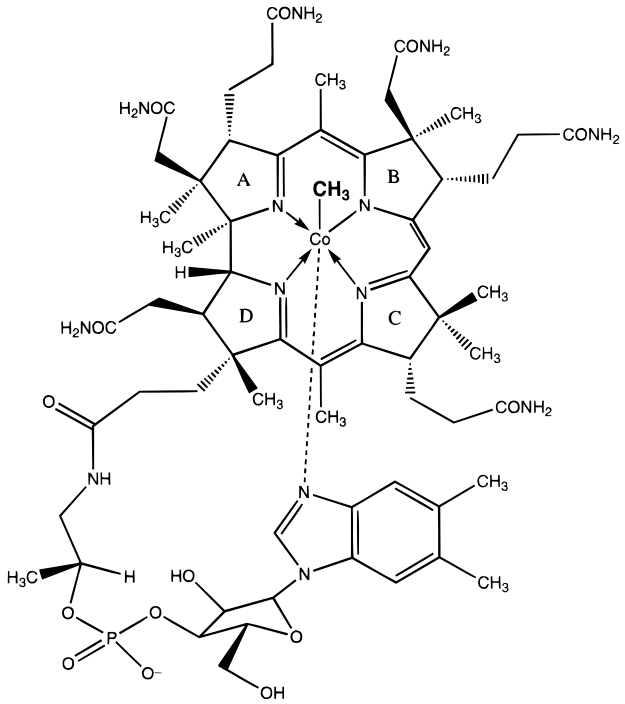

Figure 1. Structure of methylcobalamin. In adenosylcobalamin the methyl group in bold is replaced by a 5′-deoxyadenosyl group.

* To whom correspondence should be addressed.
† Department of Chemistry.
‡ Biophysics Research Division.
§ Department of Biological Chemistry.

(1) Banerjee, R. V.; Matthews, R. G. *FASEB J.* **1990**, *4*, 1450−1459.
(2) Ludwig, M. L.; Matthews, R. G. *Annu. Rev. Biochem.* **1997**, *66*, 269−313.
(3) Marsh, E. N. G. *BioEssays* **1995**, *17*, 431−441.
(4) Paul, L.; Krzycki, J. A. *J. Bacteriology* **1996**, *178*, 6599−6607.
(5) Harms, U.; Thauer, R. K. *Eur. J. Biochem.* **1996**, *241*, 149−154.
(6) Burke, S. A.; Krzycki, J. A. *J. Biol. Chem.* **1997**, *272*, 16570−16577.
(7) Drennan, C. L.; Huang, S.; Drummond, J. T.; Matthews, R. G.; Ludwig, M. L. *Science* **1994**, *266*, 1669−1674.

S0002-7863(97)04024-9 CCC: $15.00
Published on Web 04/04/1998

cofactor interactions. However, base replacement is not a universal B_{12} enzyme motif. In ribonucleotide reductase, the diol dehydratases, and ethanolamine-ammonia lyase enzymes, it appears that the DMB base provides the lower axial ligand to the cobalt.[2] In yet another enzymatic system, the corrinoid iron−sulfur protein appears to bind cobalamin in a "base-off" conformation with no nitrogenous lower axial ligand.[9]

Another important, but as yet unanswered, question in B_{12} chemistry is how carbon−cobalt bond reactivity can be directed so differently in the methyl- and adenosylcobalamin coenzymes. Theoretically the carbon−cobalt bond may cleave in three ways to form three different sets of products: (1) heterolytically where both bonding electrons remain on the cobalt to form cob(I)-alamin and a methyl cation, (2) homolytically where the electrons split between the products to form cob(II)alamin and a methyl radical, or (3) heterolytically where both bonding electrons leave with the methyl group to form cob(III)alamin and a methyl anion. In both free and enzyme-bound B_{12} cofactors all three of these cleavage patterns are observed under certain circumstances. A solid understanding of B_{12} catalysis will require detailed knowledge of the factors which influence both the relative energies of the various sets of bond-cleavage products and the pathways available for cleavage.

In recent years a variety of ultrafast laser techniques have been used to investigate bond-dissociation and recombination processes in a wide range of chemical and biological systems. In particular, time-resolved studies of ligand dissociation and rebinding in several heme proteins have proven to be very fruitful in developing a detailed understanding of a number of aspects of ligand binding and transport.[10−24] Woodruff and co-workers have reported a protein pathway for CO transport, as well as rate and equilibrium constants in cytochrome oxidase, an enzyme that catalyzes the reduction of dioxygen to water.[14] Magde and co-workers have investigated the picosecond kinetics of cytochromes b_5 and c.[11] In addition, extensive studies of myoglobin and hemoglobin have been performed.[10,12,13,15−24]

The B_{12}-dependent enzymes comprise another set of biological systems which should be amenable to productive time-resolved spectroscopic study. The UV−visible spectra of B_{12} species are well characterized and provide a useful diagnostic for oxidation state and ligation state.[25] Photolysis of both methylcobalamin and adenosylcobalamin under anaerobic conditions results in homolytic cleavage of the carbon−cobalt bond with a substantial quantum yield.[26,27] Continuous wave measurements with excitation at 442 nm determined quantum yields of $\phi = 0.20 \pm 0.03$ for adenosylcobalamin and $\phi = 0.35 \pm 0.03$ for methylcobalamin.[28] However, only a few time-resolved studies of cobalamin photolysis are reported in the literature. An early picosecond study of adenosylcobalamin revealed a nanosecond geminate recombination of the carbon−cobalt bond of sufficient magnitude to account for the low photolysis yield although the signal-to-noise ratio did not permit a precise determination of the geminate recombination rate.[29] Data on methylcobalamin were insufficient to determine whether a similar recombination occurred following photolysis of the methyl−cobalt bond. More recent measurements by Grissom and co-workers provide an estimate of the geminate recombination rate in adenosylcobalamin, (1.1 ± 0.06) ns^{-1} in aqueous solution.[30] Measurements on methylcobalamin indicated little if any geminate recombination.[31] The planar nature of the methyl radical was invoked as the most likely explanation for the lack of geminate recombination in the radical pair following photolysis of methylcobalamin. Diffusive recombination is also observed on a much longer microsecond time scale following excitation of several alkylcobalamins including methylcobalamin.[31,32]

In the present series of investigations time-resolved studies of the bond photolysis are used to investigate the reactivity of the carbon−cobalt bond in alkylcobalamins in greater detail. The results reported here establish the mechanism and quantum yields for the primary photolysis of methylcobalamin in aqueous solution. Methylcobalamin does not undergo a clean photohomolysis of the carbon cobalt bond. The present results demonstrate that excitation of methylcobalamin results in the formation of an excited state that partitions between bond homolysis ($27 \pm 3\%$) and bond heterolysis ($73 \pm 3\%$) on a subpicosecond time scale. Ground state recovery in the heterolytic channel occurs on a nanosecond time scale leaving only cob(II)alamin and methyl radical by 10 ns. The primary photochemical yield of cob(II)alamin is determined largely by the branching ratio between the two photoproduct channels.

Experimental Section

Transient Absorption Measurements. Transient absorption measurements on methylcobalamin were performed by using a tunable femtosecond laser system. A self-mode-locked Titanium Sapphire oscillator, running at 100 MHz and producing 20 fs, 2 nJ pulses, was regeneratively amplified at a kilohertz repetition rate. The resulting

(8) Mancia, F.; Keep, N. H.; Nakagawa, A.; Leadlay, P. F.; McSweeney, S. *Structure* **1996**, *4*, 339−350.
(9) Wirt, M. D.; Kumar, M.; Ragsdale, S. W.; Chance, M. R. *J. Am. Chem. Soc.* **1993**, *115*, 2146−2150.
(10) Martin, J. L.; Migus, A.; Poyart, C.; Lecarpentier, Y.; Astier, R.; Antonetti, A. *Proc. Natl. Acad. Sci. U.S.A.* **1983**, *80*, 173−177.
(11) Jongeward, K. A.; Magde, D.; Taube, D. J.; Traylor, T. G. *J. Biol. Chem.* **1988**, *263*, 6027−6030.
(12) Petrich, J. W.; Poyart, C.; Martin, J. L. *Biochemistry* **1988**, *27*, 4049−4060.
(13) Anfinrud, P. A.; Han, C.; Hochstrasser, R. M. *Proc. Natl. Acad. Sci. U.S.A.* **1989**, *86*, 8387−8391.
(14) Einarsdóttir, Ó.; Dyer, R. B.; Lemon D. D.; Killough, P. M.; Hubig, S. M.; Atherton, S. J.; López-Garriga, J. J.; Palmer, G.; Woodruff, W. H. *Biochemistry* **1993**, *32*, 12013.
(15) Chance, M. R.; Courtney, S. H.; Chavez, M. D.; Ondrias, M. R.; Friedman, J. M. *Biochemistry* **1990**, *29*, 5537−5545.
(16) (a) Alden, R. G.; Ondrias, M. R.; Courtney, S. H.; Findsen, E. W.; Friedman, J. M. *J. Phys. Chem.* **1990**, *94*, 85−90. (b) Alden, R. G.; Chavez, M. D.; Ondrias, M. R.; Courtney, S. H.; Friedman, J. M. *J. Am. Chem. Soc.* **1990**, *112*, 3241−3242.
(17) (a) Lingle, R., Jr.; Xu, X.; Zhu, H.; Yu, S. C.; Hopkins, J. B.; Straub, K. D. *J. Am. Chem. Soc.* **1991**, *113*, 3992−3994. (b) Lingle, R., Jr.; Xu, X.; Zhu, H.; Yu, S. C.; Hopkins, J. B. *J. Phys. Chem.* **1991**, *95*, 9320−9331.
(18) Schneebeck, M. C.; Vigil, L. E.; Friedman, J. M.; Chavez, M. D.; Ondrias, M. R. *Biochemistry* **1993**, *32*, 1318−1323.
(19) (a) Lim, M.; Jackson, T. A.; Anfinrud, P. A. *Proc. Natl. Acad. Sci. U.S.A.* **1993**, *90*, 5801−5804. (b) Lim, M.; Jackson, T. A.; Anfinrud, P. A. *J. Phys. Chem.* **1996**, *100*, 12043−12051.
(20) Causgrove, T. P.; Dyer, R. B. *Biochemistry* **1993**, *32*, 11985−11991.
(21) Walda, K. N.; Liu, X. Y.; Sharma, V. S.; Magde, D. *Biochemistry* **1994**, *33*, 2198−2209.
(22) Lian, T.; Locke, B.; Kholodenko, Y.; Hochstrasser, R. M., *J. Phys. Chem.* **1994**, *98*, 11648−11656.
(23) Jackson, T. A.; Lim, M.; Anfinrud, P. A. *Chem. Phys.* **1994**, *180*, 131−140.
(24) Lim, M.; Jackson, T. A.; Anfinrud, P. A. *Science* **1995**, *269*, 962−966.
(25) Giannotti, C. In *B_{12}*; Dolphin, D., Ed.; John Wiley and Sons: New York, 1982; Vol. 1, pp 393−430.
(26) Hogenkamp, H. P. C. In *B_{12}*; Dolphin, D., Ed.; John Wiley and Sons: New York, 1982; Vol. 1, pp 295−323.
(27) Pratt, J. M.; Whitear, B. R. D. *J. Chem. Soc. (A)* **1971**, 252−255.
(28) Chen, E.; Chance, M. R. *Biochemistry* **1993**, *32*, 1480−1487.
(29) Endicott, J. F.; Netzel, T. L. *J. Am. Chem. Soc.* **1979**, *101*, 4000−4002.
(30) Chagovetz, A. M.; Grissom, C. B. *J. Am. Chem. Soc.* **1993**, *115*, 12152−12157.
(31) Lott, W. B.; Chagovetz, A. M.; Grissom, C. B. *J. Am. Chem. Soc.* **1995**, *117*, 12194−12201.
(32) Chen, E.; Chance, M. R. *J Biol Chem* **1990**, *265*, 12987−12994.

laser beam was centered at approximately 800 nm, providing 400 μJ, 70 fs pulses at a repetition rate of 1 kHz. The pump and probe beams were produced by splitting the amplified Ti:sapphire output using a 50−50 beam splitter. The pump pulses were delayed with respect to the probe pulses by a computer-controlled motorized translation stage. The pump pulses at 400 nm were generated by frequency doubling in a 300 μm β-barium borate (BBO) crystal. A Schott glass BG-39 filter was used to remove the residual fundamental. This produced pump pulses with pulse energies of ca. 40 μJ. Neutral density filters were used to further reduce the pump energy to ca. 2 μJ/pulse.

A visible white light continuum was generated for use as a probe beam by focusing the fundamental into flowing ethylene glycol. For measurement of the fast kinetic components the continuum was generated in a 200 μm ethylene glycol jet in order to preserve the pulse width. For long time scale kinetic measurements and spectral measurements in which stability was the greater issue, the continuum was generated in a 1 cm ethylene glycol flow cell. In addition, a near-UV continuum extending to ca. 300 nm was generated by focusing the second harmonic of the laser into a 3 mm sapphire window. For kinetic measurements at specific wavelengths the desired wavelength was selected by using a set of interference filters (full width at half-maximum of 10 nm). A reference beam was obtained by ca. 4% reflection off of a glass slide, while the remaining 96% was focused into the sample as the signal beam. Kinetic data were recorded as described previously.[33] Isotropic kinetic data were obtained by rotating the polarization of the pump beam to magic angle (54.7°) with respect to the polarization of the probe beam, or were constructed from individual parallel and perpendicularly polarized kinetic traces as

$$I_{iso}(t) = {}^1/_3[I_{||}(t) + 2I_{\perp}(t)] \quad (1)$$

For the measurement of transient difference spectra the setup was modified to use spherical mirrors at near normal incidence to collect and focus the probe. This was done to minimize chromatic aberration obtained with refractive optics. The probe beam was rotated to vertical polarization and the pump beam was rotated to magic angle so that only isotropic data were collected. The continuum and the pump pulse were focused to about 500 μm. After passing through the sample, the probe beam was focused onto an optical fiber connected to a SPEX 500M spectrometer with a Princeton Instruments Model LN/CCD-1100-PB CCD camera. Each camera exposure was 250 ms in duration, and 5000 exposures were typically collected. To obtain a difference spectrum a solenoid with a shutter was timed to block the pump beam every other time the camera shutter closed. The difference spectra were calculated by averaging every other exposure to obtain a pumped average while the remaining 2500 exposures were averaged to give a reference. Taking the common log of the ratio then gave the recorded spectra.

Sample Preparation. Methylcobalamin was obtained from Sigma and used without further purification. The samples were prepared and kept under anaerobic conditions. This was done by bubbling nitrogen through double distilled, deionized water for a minimum of 1 h after which ca. 2 mM solutions were made. The samples were placed in a reservoir and kept under nitrogen. The reservoir was placed in an ice bath to prevent thermal degradation. The solutions were flowed through a 1 mm path length cell with a rate sufficient to ensure the illuminated volume was refreshed between pulses. The pH of the methylcobalamin samples was 6.9 and the solutions were not buffered. UV−visible spectra of the samples obtained before and after laser exposure were the same.

Steady-State Spectral Measurements. Steady-state absorption spectra of cobalamin samples in varying ligation states and oxidation states were recorded on a Hewlett-Packard 8453 diode-array spectrophotometer equipped with a temperature-controlled cuvette holder and with a 270 nm filter to minimize UV damage to the sample. Steady-state spectra of methylcobalamin, cob(II)alamin, cob(I)alamin, aquocob(III)alamin, and hydroxocob(III)alamin are shown in Figure 2. Methylcobalamin (40 μM) was prepared in 10 mM potassium phosphate buffer at pH 7.2. Hydroxocob(III)alamin (20 μM) was prepared in 10 mM Tris−HCl at pH 9.0. Cob(II)alamin was prepared by slow photolysis of a sample of methylcobalamin (40 μM) in the presence of TEMPO (500 μM) in 10 mM potassium phosphate buffer at pH 7.2 under an argon atmosphere. Cob(I)alamin was prepared by reduction of a sample of hydroxocob(III)alamin (20 μM) with a 2-fold excess of titanium(III) citrate in 10 mM Tris−HCl at pH 7.2 under an argon atmosphere. The steady-state spectra in Figure 2 are scaled to literature values of the maximum molar extinction coefficients.[34]

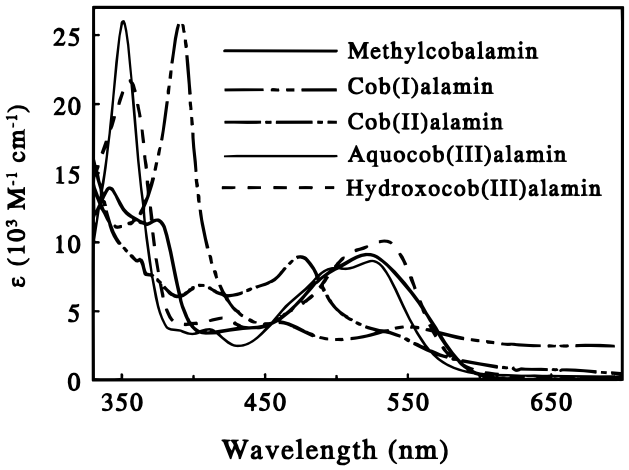

Figure 2. Steady-state spectra of methylcobalamin, cob(I)alamin, cob(II)alamin, hydroxocob(III)alamin, and aquocob(III)alamin. The spectra have been scaled by using literature values of ϵ_{max}.[34]

Transient difference spectra were analyzed by comparison with steady state difference spectra generated as described below. The difference spectrum for the conversion of methylcobalamin to hydroxocob(III)alamin was generated by slow photolysis of a sample of methylcobalamin (20 μM) and TEMPO in air-saturated 10 mM Tris−HCl at pH 9.0. Photolysis was achieved with a 150 W tungsten lamp held 10 in. above the sample while spectra were recorded every 2 min for 1 h. The difference between successive spectra was calculated, scaled to the extinction coefficients calculated from Figure 2, and averaged. The difference spectrum for conversion of methylcobalamin to cob(II)alamin was generated by using the same procedure, except that the sample of methylcobalamin and TEMPO was prepared in 10 mM potassium phosphate buffer at pH 7.2 under an argon atmosphere.

Results

Transient Absorption Data. Transient kinetic measurements were made at 12 wavelengths between 400 and 730 nm. Typical kinetic measurements for 540, 570, and 600 nm are shown in Figure 3. The kinetic data were analyzed by fitting the traces to a sum of exponentials in a global analysis. This analysis required the inclusion of four decay components and a nondecaying component. The time constants obtained from the fitting procedure are $\leq$0.3 ps, 3.4 $\pm$ 0.5 ps, 22 $\pm$ 2 ps, and 1.2 $\pm$ 0.5 ns. Accurate assignment of these kinetic components to physical processes requires more detailed information on the spectral behavior.

Visible transient absorption difference spectra were obtained for a variety of delay times between 1 ps and 9 ns. The evolution of the spectrum from 0.5 to 40 ps is illustrated by the data shown in Figure 4. The difference spectrum is well-developed within 1 ps, with only relatively minor changes observed between 1 and 40 ps. Visible transient absorption difference spectra obtained for time delays of 40 ps, 900 ps, and 9 ns after excitation are shown in Figure 5. The steady

(33) Pullen, S.; Walker, L. A., II; Sension, R. J. *J. Chem. Phys.* **1995**, *103*, 7877−7886.

(34) (a) Hill, J. A.; Pratt, J. M.; Williams, R. J. P. *J. Chem. Soc.* **1964**, 5149−5153. (b) Hill, H. A. O.; Pratt, J. M.; Williams, R. J. P. *Proc. R. Soc.* **1965**, *A288*, 362.

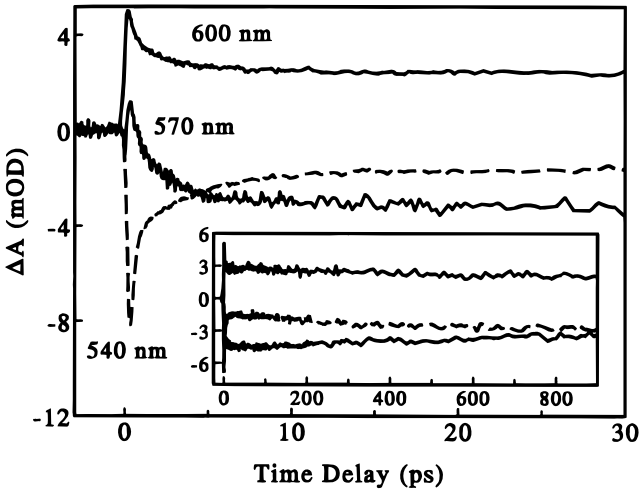

Figure 3. Picosecond transient absorption kinetics at 600 nm (positive solid line), 570 nm (negative solid line), and 540 nm (dashed line). The fast kinetic components involve internal conversion and bond breaking. The spectral changes have stabilized by 20 ps. Further spectral changes occur on a much longer time scale as shown in the inset.

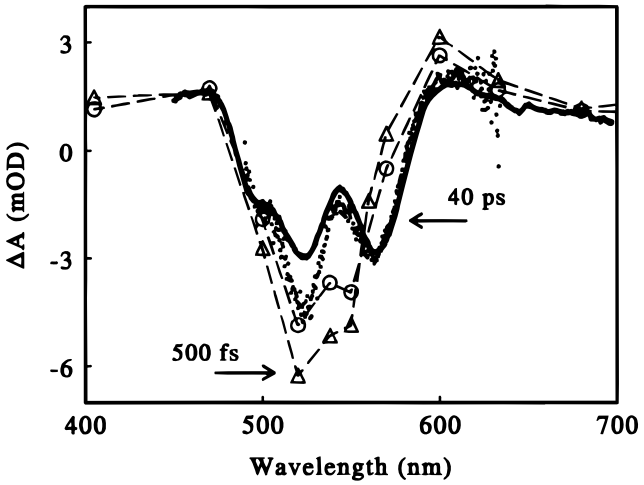

Figure 4. Evolution of the transient difference spectrum following excitation of methylcobalamin from 500 fs to 40 ps. Transient absorption difference spectra are plotted for 5 ps (filled dots) and 40 ps (dark line). These data were obtained by using a broad band continuum and a CCD camera. The difference spectra at 500 fs (open triangles) and 1.0 ps (open circles) were obtained from the kinetic behavior observed at specific wavelengths (as shown in Figure 3). The transient difference spectrum is well established within 1 ps, with small amplitude changes between 1 and 40 ps characteristic of relaxation processes.

state difference spectrum expected for a cob(II)alamin photoproduct is also shown in this latter figure. The 9 ns difference spectrum is consistent with a homolytic bond cleavage as expected from steady-state measurements.[26,27,32,35−37] The spectra obtained at earlier delay times on the other hand are substantially different.

The transient absorption difference spectrum at a delay of 40 ps was also obtained over several spectral windows. These data are shown in Figure 6. The spectral region between 380 and 450 nm was obtained by using orthogonally polarized pump and probe beams in order to filter out the pump pulse. The remaining data were obtained with a magic angle polarization geometry. A visible transient absorption difference spectrum obtained at pH 8.3 for a delay time of 40 ps differs only very slightly from the spectrum obtained at pH 6.9. Finally, a transient absorption difference spectrum for methylcobalamin

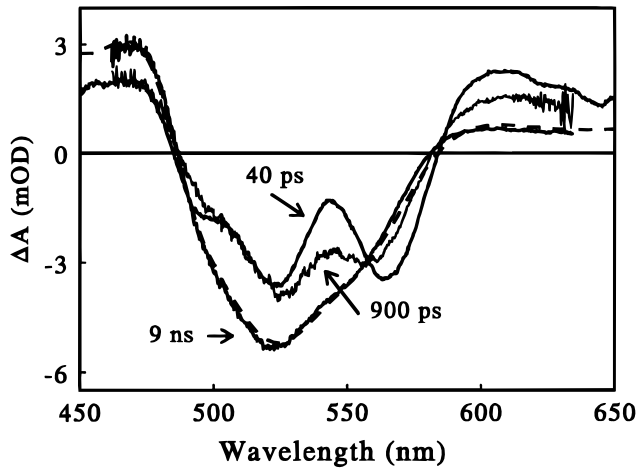

Figure 5. Transient difference spectra obtained at 40 ps, 900 ps, and 9 ns, as labeled. The smooth dashed line represents the difference spectrum expected for bond homolysis forming cob(II)alamin.

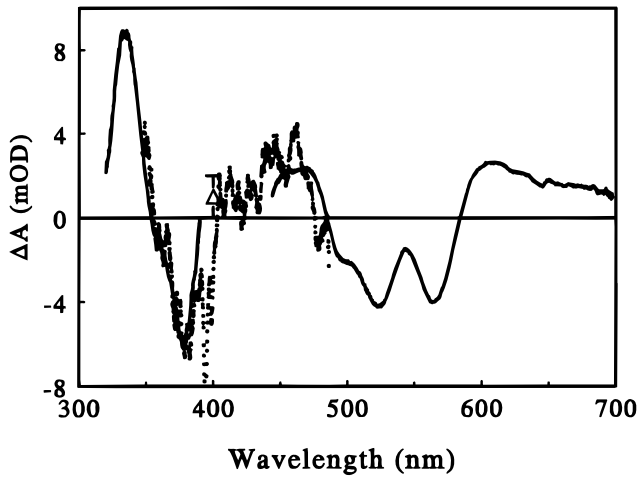

Figure 6. Transient difference spectra obtained at 40 ps. The solid lines were obtained by using magic angle polarization. The spectrum around 400 nm (dots) was obtained by using perpendicular polarization to minimize contamination by the pump pulse. Some pump pulse has scattered into the spectrometer as indicated by the dip at 400 nm. A separate one-color kinetic measurement (indicated by the data point with error bar) determined that the absorbance change at 400 nm is always positive.

bound to methionine synthase was obtained for a delay time of 40 ps. This difference spectrum is quite similar to that observed for the free cofactor in aqueous solution.

Singular Value Decomposition Analysis. The visible transient absorption difference spectra obtained between 40 ps and 9 ns were subjected to analysis by using a singular value decomposition (SVD) algorithm.[38] The SVD algorithm produced six basis spectra, two of which contained signal, while the remaining four were dominated by noise, containing no significant signal. Retaining only the two significant basis spectra, the SVD output was used to generate the species associated difference spectra shown in Figure 7. As required

(35) Schrauzer, G. N.; Lee, L. P.; Sibert, J. W. *J. Am. Chem. Soc.* **1970**, *92*, 2997−3005.
(36) Schrauzer, G. N.; Sibert, J. W.; Windgassen, R. J. *J. Am. Chem. Soc.* **1968**, *90*, 6681−6688.
(37) Taylor, R. T.; Smucker, L.; Hanna, M. L.; Gill, J. *Arch. Biochem. Biophys.* **1973**, *156*, 521−533.
(38) Henry, E. R.; Hofrichter, J. *Methods in Enzymol.* **1992**, *210*, 129−192.

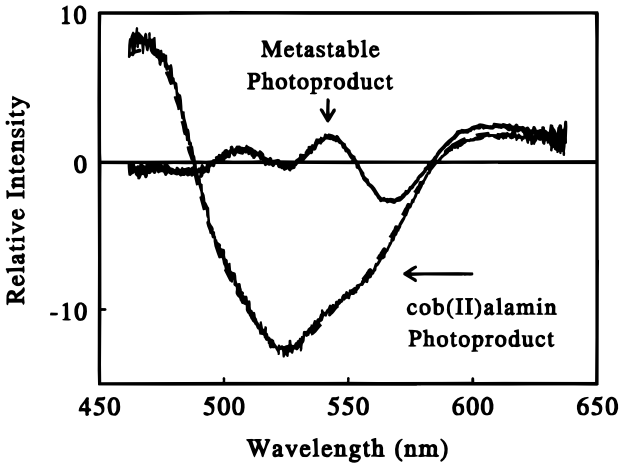

Figure 7. Species associated difference spectra obtained in the singular value decomposition analysis. The dashed line is a steady state difference spectrum for the formation of cob(II)alamin from methylcobalamin.

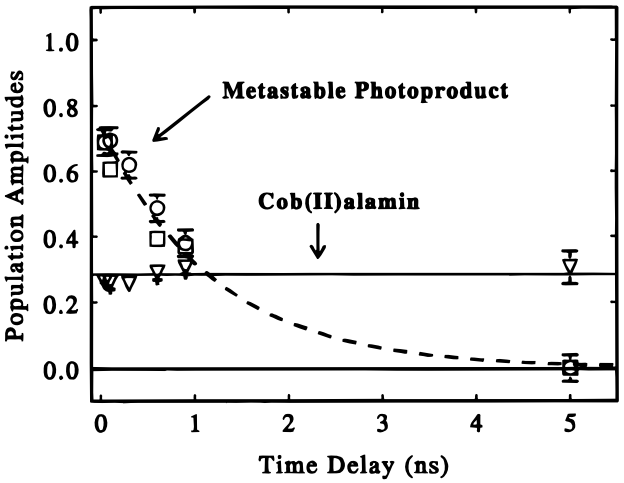

Figure 8. Population of the two photoproducts as a function of time following excitation. The circles and triangles represent the populations of the cob(III)alamin and cob(II)alamin photoproducts, respectively, as derived from a least-squares fit of the species associated spectra to the transient difference spectrum. The squares and crosses represent the population vectors for the cob(III)alamin and cob(II)alamin photoproducts, respectively, as obtained directly from the SVD analysis. The dashed line represents single-exponential decay of 1.2 ns as determined from the individual kinetic measurements.

from steady-state photolysis experiments and from the 5 and 9 ns spectra obtained in the present study, one of these species associated spectra corresponds to the difference spectrum resulting from the formation of cob(II)alamin from methylcobalamin. The difference spectrum corresponding to the second species is relatively small, indicating that this species has a spectrum similar to that of the methylcobalamin precursor.

The treatment of the SVD basis spectra to yield species associated spectra also permits the calculation of population vectors describing the temporal behavior of the populations of the two species. These vectors are plotted in Figure 8 (squares and crosses). Because only two of the initial six basis spectra were retained, the population vectors obtained from the SVD do not necessarily (i.e. mathematically) represent the best fit to the experimental data in a least-squares sense. Therefore the two species associated basis spectra were also used to fit the experimental transient absorption difference spectra and obtain the best least-squares population amplitudes for each time point. These amplitudes are plotted in Figure 8 (circles and triangles).

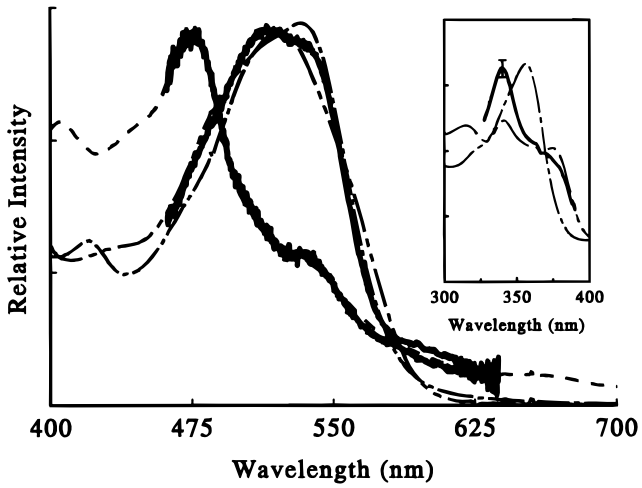

Figure 9. Visible absorption spectra of the two photoproducts (solid lines). The dashed line is the steady-state spectrum of cob(II)alamin, the dot-dashed line is the spectrum of hydroxocobalamin, and the double-dot dashed line is the spectrum of methylcobalamin. The inset shows the UV spectrum of the metastable photoproduct as deduced from the 40 ps transient difference spectrum by assuming that only two components contribute. Again in the inset, the double-dot-dashed line is the steady-state spectrum of methylcobalamin, while the dot-dashed line is the spectrum of hydroxocobalamin. The error bar on the peak absorption at 340 nm represents the reliability of the peak intensity derived from the decomposition.

The decay of the metastable (noncob(II)alamin) photoproduct is well modeled by an exponential decay with a time constant of 1.4 ns (from the least-squares fit to the basis spectra) or 1.1 ns (from the SVD analysis with no post-analysis). These estimates for the decay are consistent with the 1.2 ns time constant obtained through the global analysis of the transient kinetic data. The population of the cob(II)alamin photoproduct is essentially time-independent between 40 ps and 9 ns following photolysis. The population of cob(II)alamin (i.e., quantum yield for homolysis) is 0.27 ± 0.03 between 40 and 900 ps. It is possible that a small portion of the second photoproduct decays to form cob(II)alamin and a methyl radical, but the majority ($\geq$85%) decays to form ground electronic state methylcobalamin (difference spectrum $\Delta A \equiv 0$).

Photoproduct Spectra. The species associated difference spectra obtained in the present SVD analysis can be used, along with the steady-state spectrum of methylcobalamin, to construct the absorption spectra of the two photoproducts formed following excitation of methylcobalamin. The amplitude of the methylcobalamin bleach is dictated by comparison of the transient cob(II)alamin difference spectrum with the steady state difference spectrum. The spectra of the two photoproducts are plotted in Figure 9 along with steady-state spectra of methylcobalamin, cob(II)alamin, and hydroxocob(III)alamin. The second photoproduct has an absorption spectrum with a visible absorption band ($\alpha\beta$ band) characteristic of a cob(III)alamin species either with a covalent bond to the upper axial group as in alkylcobalamins or ligated as in aquo- or hydroxocob(III)alamin. However, the cob(III)-like photoproduct has an additional, relatively intense, red-shifted absorption wing.

The visible $\alpha\beta$ absorption band of a cob(III)alamin species depends on the nature of the axial ligand in a manner which is, as yet, rather poorly characterized. The γ-band region between 300 and 400 nm is a much more useful diagnostic feature. The 40 ps difference spectrum shown in Figure 6 may be used to reconstruct the spectrum of the cob(III)-like photoproduct in the near-UV region. This 40 ps difference spectrum signal is

given by:

$$\Delta A(\nu) = \sigma_{Co(II)}P_{Co(II)} + \sigma_{MS}P_{MS} - \sigma_{MC}(P_{Co(II)} + P_{MS}) \quad (2)$$

where the absorption spectra of cob(II)alamin ($\sigma_{Co(II)}$) and methylcobalamin (σ_{MC}) are known from steady-state measurements and the populations of cob(II)alamin ($P_{Co(II)}$) and the metastable photoproduct (P_{MS}) were determined in the SVD analysis. The photoproduct spectrum (σ_{MS}) is constructed by adding the methylcobalamin spectrum to the measured difference spectrum and subtracting the contribution arising from the formation of cob(II)alamin. The near-UV absorption spectrum of the metastable photoproduct is shown in the inset in Figure 9 and compared with the steady-state spectra of methylcobalamin and hydroxocobalamin. The photoproduct spectrum is characteristic of a cob(III)alamin species in both the visible and near-UV regions of the spectrum. A γ-band absorption feature is clearly identified, peaking at 340 nm, with an intensity comparable to the γ-band intensity in hydroxocobalamin.

The lone assumption inherent to this reconstruction is that only two species (cob(II)alamin and the cob(III)-like photoproduct) contribute to the transient difference spectrum at 40 ps. This assumption is supported by several observations: (1) The SVD decomposition of the visible transient difference spectrum produces only two significant basis spectra implying that only two components contribute to the transient absorption in the visible. (2) The populations obtained in the SVD analysis indicate that the cob(II)alamin concentration is time-independent and accounts for ca. 27% of the total photolysis. (3) The quantum yield for photolysis of methylcobalamin is reported in the literature to fall between 0.28 and 0.35 following excitation at wavelengths near 400 nm.[27,28,37] Comparison of the relative population of cob(II)alamin in the present spectral measurements with the reported steady-state yields suggests that the two species identified in the SVD decomposition of the visible transient absorption difference spectra are the only significant photolysis products. The presence of a third photoproduct would decrease the cob(II)alamin quantum yield to a value inconsistent with the quantum yield obtained in steady-state measurements.

Discussion

It has been suggested that excitation of methylcobalamin results in the formation of an excited state that partitions between bond homolysis (formation of a {cob(II)alamin$\cdots{}^{\bullet}CH_3$} radical pair) and internal conversion to the ground state followed by vibrational relaxation.[39,40] However, the transient absorption difference spectra presented here indicate that a metastable cob(III)alamin photoproduct is produced in addition to the stable cob(II)alamin photoproduct. The spectrum of this intermediate (Figure 9) is characteristic of a cob(III)alamin species. It is well established that the wavelength of the γ-band correlates with ligand strength.[25] A strong ligand produces a red-shifted γ-band while a weak ligand produces a blue-shifted γ-band. The spectra shown in Figure 2 demonstrate this trend, the γ-band of aquocobalamin (water being a weak ligand) is located at 350 nm while the γ-band of hydroxocobalamin (OH^- being a relatively strong ligand) is located at 356 nm. For comparison, vitamin B_{12} has a strong cyano (CN^-) ligand and a γ-band located at 361 nm. Finally, the lone pair of electrons in cob(I)alamin may be considered to represent the ultimate in strong ligands, with the resulting γ-band located at 391 nm. The γ-band of the metastable cob(III)alamin species produced by photolysis is located at 340 nm, implying a particularly weak axial ligand. A probable assignment for the metastable photoproduct is an ion pair consisting of five-coordinate cob(III)alamin and a methyl anion. It should be realized, however, that the metastable photoproduct might be an intact methylcob(III)alamin molecule with a very long, weak C−Co bond. If cob(I)alamin represents the ultimate in strong ligands, the present metastable photoproduct may represent the ultimate in weak ligands.

The present results suggest that excitation of methylcobalamin results in the formation of an excited state which partitions between bond homolysis (formation of a {cob(II)alamin$\cdots{}^{\bullet}CH_3$} radical pair) and bond heterolysis (formation of a {cob(III)alamin$\cdots{}^{-}CH_3$} ion pair) on a subpicosecond time scale. The 3.4 and 22 ps kinetic components observed in the transient kinetic measurements are best assigned to minor spectral evolution resulting from vibrational and conformational relaxation following bond cleavage. The overall spectral changes observed between 1 and 40 ps are relatively small (see Figure 4 and Supporting Information). The essential features of the photoproduct difference spectrum are well developed within the first picosecond following excitation.

The competition between homolysis and heterolysis observed in the present study is not unique to the photochemistry of cobalamin compounds. A competition between homolytic and heterolytic cleavage is also observed in the thermolysis of alkylcobalamins.[41−43] In addition, theoretical calculations of bond cleavage in model systems predict that the stretched C−Co bond may dissociate to form either Co(III) + C^- or Co(II) + $^{\bullet}C$.[44,45] The relative energies of the two product states depend on the nature of the alkyl ligand and the nature of the transaxial ligand. The ultimate photolysis, and presumably thermolysis, quantum yields depend on the relative energies of the product states, and on the rate of geminate recombination for each pair of products. The present measurements suggest that the relative energies of the two sets of photoproducts are similar and either may be produced. However, geminate recombination between cob(III)alamin and the methyl anion occurs with near unity quantum yield. Thus, heterolytic cleavage is not observed in steady-state photolysis measurements. The high quantum yield for geminate recombination of cob(III)alamin and the methyl anion is consistent with the fact that, unlike the methyl radical, the methyl anion will maintain a tetrahedral geometry suitable for prompt recombination.

The Photolysis of Methylcobalamin in Methionine Synthase. Photolysis of methylcobalamin has been used to probe the effects of mutations on the structure and reactivity of methionine synthase.[39,40] In addition, protection from photolysis has been proposed as a function of the transport protein cobalophilin.[46] Photolysis can be inhibited in the protein environment in several ways, four of which are enumerated

(39) Jarrett, J. T.; Amaratunga, M.; Drennan, C. L.; Scholten, J. D.; Sands, R. H.; Ludwig, M. L.; Matthews, R. G. *Biochemistry* **1996**, *35*, 2464−2475.

(40) Jarrett, J. T.; Drennan, C. L.; Amaratunga, M.; Scholten, J. D.; Ludwig, M. L.; Matthews, R. G. *Bioorg. Med. Chem.* **1996**, *4*, 1237−1246.

(41) Garr, C. D.; Sirovatka, J. M.; Finke, R. G. *Inorg. Chem.* **1996**, *35*, 5912−5922.

(42) Garr, C. D.; Sirovatka, J. M.; Finke, R. G. *J. Am. Chem. Soc.* **1996**, *118*, 11142−11145.

(43) Sirovatka, J. M.; Finke, R. G. *J. Am. Chem. Soc.* **1997**, *119*, 3057−3067.

(44) Mealli, C.; Sabat M.; Marzilli, L. G. *J. Am. Chem. Soc.* **1987**, *109*, 1593−1594.

(45) Hansen, L. M.; Kumar, P. N. V. P.; Marynick, D. S. *Inorg. Chem.* **1994**, *33*, 728−735.

(46) Frisbie, S. M.; Chance, M. R. *Biochemistry* **1993**, *32*, 13886−13892.

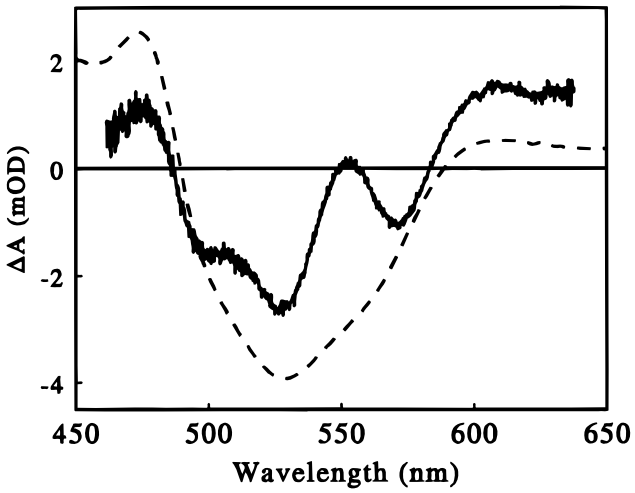

Figure 10. Transient difference spectra obtained at 40 ps following excitation of methylcobalamin bound to methionine synthase. The smooth dashed line represents the difference spectrum expected for bond homolysis forming cob(II)alamin. The peak observed in the transient difference spectrum at 552 nm clearly indicates the formation of metastable cob(III)alamin.

here: (1) The cage effect of the protein will increase the recombination probability by preventing escape of the methyl radical. (2) The protein may exclude oxygen from the cobalamin binding pocket, preventing oxidation of the methyl radical, and thereby increasing the relative yield of methyl recombination. (3) The protein may affect the structure of cob(II)alamin, increasing the recombination probability. (4) The protein may alter the primary photochemical yield of cob(II)alamin. Any combination of these effects is also possible.

Studies of a series of methionine synthase mutants affecting the cap over the methyl-binding face of cobalamin have demonstrated that the protein does indeed provide a cage that enhances recombination by preventing escape of the methyl radical.[39] This is not the only influence, however. Mutation of His 759 (the lower cobalt ligand) to glycine increases the rate of photolysis substantially.[40] Mutations of Asp 757 and Ser 810, which are coupled to His 759 and thus the cobalamin cofactor, by a chain of hydrogen bonds, also increase the rate of photolysis, although by much smaller amounts.[40] These measurements suggest that in addition to providing a radical cage, the protein also alters either the structure of cob(II)alamin or the primary photochemical yield.

The present series of measurements on free methylcobalamin in aqueous solution demonstrates that the ultimate photochemical yield of cob(II)alamin is determined by the branching ratio between homolytic and heterolytic photolysis channels within a picosecond. In light of this result, it is reasonable to propose that the protein may alter the photolysis rate of enzyme-bound methylcobalamin by altering the branching ratio between the cob(III)alamin and cob(II)alamin channels and inhibiting the initial formation of cob(II)alamin. One possible hypothesis is that the axial histidine ligand in methionine synthase acts to inhibit photoinduced homolysis and promote heterolysis.

To investigate this possibility, we have obtained a transient difference spectrum of enzyme bound methylcobalamin 40 ps after excitation at 400 nm [Figure 10]. This spectrum clearly shows formation of cob(III)alamin as evidenced by the peak at 552 nm. The major differences between the transient absorption difference spectrum of the free cofactor and the enzyme-bound cofactor may be attributed to changes in the steady-state absorption spectra of cob(II)alamin and methylcobalamin bound to methionine synthase. The difference spectrum observed for the enzyme-bound cofactor indicates a photolysis yield of ca. 30% for cob(II)alamin. Within experimental error the branching ratio does not appear to be affected by interaction with the protein. Future work will explore the branching ratio and geminate recombination in greater detail through a full transient absorption study.

Conclusions

The present paper reports a spectroscopic investigation of the photolysis and recombination of methylcobalamin. Methylcobalamin does not undergo a clean photohomolysis of the carbon−cobalt bond. The most consistent interpretation of the data reported here is that ca. 27% of the initially excited methylcobalamin undergoes a bond homolysis on a subpicosecond time scale. The remaining 73% forms a metastable cob(III)alamin photoproduct. This latter channel suggests that methylcobalamin undergoes a heterolytic bond-cleavage with a quantum yield of ca. 0.73, forming a metastable complex with cob(III)alamin and a methyl anion. Previous transient absorption measurements missed the formation and recombination of cob(III)alamin because of an inadequate signal-to-noise ratio. The pioneering picosecond measurement by Endicott and Netzel[29] involved kinetic measurements at 474 and 565 nm. The precision of these data, the difficulty of the experiment, and the limited number of data points prohibited identification of the actual photoproducts. The picosecond measurements of Lott et al. integrated the transient absorption intensity centered at 471 nm.[31] The present analysis predicts that the average cob(III)alamin difference spectrum in this region is zero. Therefore, integration in this region will yield a nondecaying signal correctly attributed to the formation of cob(II)alamin.

Recombination in the heterolytic photolysis channel occurs exponentially on a time scale of 1.2 ± 0.5 ns leaving essentially cob(II)alamin and methyl radical by 10 ns. The photochemical yield of cob(II)alamin is determined primarily by the branching ratio between the homolytic and heterolytic dissociation channels within approximately 1 ps of excitation.

The 40 ps transient absorption difference spectrum of methylcobalamin bound to methionine synthase indicates that the branching ratio and initial production of cob(II)alamin is not changed substantially in the enzyme-bound cofactor. The substantial photolysis protection afforded by the enzyme must be attributed to processes which enhance recombination, by caging the methyl radical to prevent escape and by increasing the intrinsic rate of recombination.

Acknowledgment. This research was supported in part by NIH GM24908 (R.G.M.). J.T.J. was supported in part by an NIH postdoctoral fellowship F32 GM17455. S.H.P. was supported by the Center for Ultrafast Optical Sciences (NSF-STC-PHY-8920108).

Supporting Information Available: Transient difference spectra after excitation at 400 nm (Figure A) and evolution of the transient difference spectrum (Figure B) (2 pages, print/PDF). See any current masthead for ordering instructions and Web access information.

JA974024Q